# Spatiotemporal modelling of hormonal crosstalk explains the level and patterning of hormones and gene expression in *Arabidopsis thaliana* wildtype and mutant roots

Simon Moore[1*], Xiaoxian Zhang[2*], Anna Mudge[1], James Rowe[1], Jennifer F. Topping[1], Junli Liu[1†] and Keith Lindsey[1†]

[1]The Integrative Cell Biology Laboratory, School of Biological and Biomedical Sciences, Durham University, South Road, Durham DH1 3LE, UK

[2] School of Engineering, The University of Liverpool, Brownlow Street, Liverpool L69 3GQ, UK

[*]Joint first authors: both authors contributed equally to this work.

[†]Joint corresponding authors

Junli Liu: Junli.Liu@durham.ac.uk

Keith Lindsey: Keith.Lindsey@durham.ac.uk

Author for correspondence: Keith Lindsey (keith.lindsey@durham.ac.uk, tel: +44 191 334 1309 fax: +44 191 334 1201).

Junli Liu ( Junli.Liu@durham.ac.uk, tel: +44 191 3341376)

Running title: Patterning of hormones and gene expression in *Arabidopsis*

| | | | |
|---|---|---|---|
| Total word count (Introduction, M&M, Results, Discussion): | **6993** | No. of figures: | **9** |
| Summary: | **197** | No. of Tables: | **0** |
| Introduction: | **795** | No. of Supporting Information files: | **1** |
| Materials and Methods: | **855** | Discussion: | **1827** |
| Results: | **3516** | Acknowledgements: | **33** |

**Summary**

- Patterning in *Arabidopsis* root development is coordinated via a localized auxin concentration maximum in the root tip, requiring the regulated expression of specific genes. However, little is known about how hormone and gene expression patterning is generated.
- Using a variety of experimental data, we develop a spatiotemporal hormonal crosstalk model that describes the integrated action of auxin, ethylene and cytokinin signalling, the POLARIS protein, and the functions of PIN and AUX1 auxin transporters. We also conduct novel experiments to confirm our modelling predictions.
- The model 1) reproduces auxin patterning and trends in wild-type and mutants; 2) reveals that coordinated PIN and AUX1 activities are required to generate correct auxin patterning; 3) correctly predicts shoot to root auxin flux, auxin patterning in the *aux1* mutant, the levels of cytokinin, ethylene and PIN protein, and PIN protein patterning in wild-type and mutant roots. Modelling analysis further reveals how PIN protein patterning is related to the POLARIS protein through ethylene signalling. Modelling prediction on the patterning of *POLARIS* expression is confirmed experimentally.
- Our combined modelling and experimental analysis reveals that a hormonal crosstalk network regulates the emergence of patterns and levels of hormones and gene expression in wild-type and mutants.

Key words: hormonal crosstalk, mathematical modelling, mutant roots, patterning of auxin, PIN proteins, PLS peptide, root development.

## INTRODUCTION

*Arabidopsis* root development and response to varying environmental conditions involves a complex network of overlapping interactions between plant signalling hormones and gene expression known as 'hormonal crosstalk'. Hormone concentrations in the cells are a function of multiple factors such as hormone biosynthesis, long and short range transport, rate of influx and efflux by carrier proteins, and hormone activation, inactivation and degradation (e.g. Weyers & Paterson, 2001; Del Bianco *et al*., 2013). Hormones and the associated regulatory and target genes form a network, in which relevant genes regulate hormone activities and hormones regulate gene expression (Chandler, 2009; Bargmann *et al*., 2013; Depuydt & Hardtke, 2011; Vanstraelen & Benkov, 2012). For example, auxin biosynthesis is stimulated by ethylene and inhibited by cytokinins (Eklof *et al*., 1997; Nordstrom *et al*., 2004; Ruzicka *et al*., 2007; Swarup *et al*., 2007; Stepanova *et al*., 2007.) and *PIN1* and *PIN2* mRNA and protein levels are promoted by auxin and ethylene (Paciorek *et al*., 2005; Vanneste & Friml, 2009) and inhibited by cytokinin (Ruzicka *et al*., 2009). Therefore, root development is controlled by a hormonal crosstalk network that integrates gene expression, signal transduction and the metabolic conversion complexities associated with hormonal crosstalk activity (Liu *et al*. 2014).

Hormone signalling and gene expression responses are patterned to regulate correct root development. Cellular patterning in the *Arabidopsis* root is coordinated in part via a localized auxin concentration maximum close to the quiescent centre (QC, Sabatini *et al*., 1999), which regulates the expression of specific genes such as the *PLETHORA* family (Aida *et al*. 2004) and *WOX5* (Sarkar *et al*. 2007). This auxin gradient has been hypothesized to be sink-driven (Friml *et al*., 2002) and computational modelling suggests that auxin efflux carrier permeability may be sufficient to generate the gradient in the absence of auxin biosynthesis in the root (Grieneisen *et al*., 2007; Wabnik e*t al*., 2010; Clark *et al*. 2014). Genetic studies show that auxin biosynthesis (Ikeda *et al*., 2009; Tivendale *et al*., 2014; Zhao, 2010), the AUX1/LAX influx carriers (Swarup *et al*., 2005, 2008; Jones *et al*., 2008; Krupinski & Jonsson, 2010; Band *et al*., 2014.), and the PIN auxin efflux carriers (Petrásek *et al*., 2006; Grieneisen *et al*., 2007; Krupinski & Jonsson, 2010; Mironova *et al*., 2010.) all play important roles in the formation of auxin gradients. Recently, it has also been demonstrated that growth and patterning during vascular tissue formation in *Arabidopsis* results from an integrated genetic network controlling tissue development (De Rybel *et al*. 2014).

Auxin concentration is regulated by diverse interacting hormones and gene expression and therefore cannot change independently of the various crosstalk components in space and time; similarly,

ethylene and cytokinin concentrations and expression of the associated regulatory and target genes are also interlinked (e.g. To *et al*., 2004; Shi *et al*., 2012). Important questions for understanding hormonal crosstalk in root development include a) how hormone concentrations and expression of the associated regulatory and target genes are mutually related and b) how patterning of both hormones and gene expression emerges under the action of hormonal crosstalk. We previously developed a hormonal interaction network for a single *Arabidopsis* cell by iteratively combining modelling with experimental analysis (Liu *et al*., 2010, 2013). We described how such a network regulates auxin concentration in the *Arabidopsis* root by controlling the relative contribution of auxin influx, biosynthesis and efflux, and by integrating auxin, ethylene and cytokinin signalling as well as PIN and POLARIS (PLS) peptide function. The *PLS* gene of *Arabidopsis* transcribes a short mRNA encoding a 36-amino acid peptide that is required for correct root growth and vascular development (Casson *et al*., 2002). Experimental evidence shows that there is a link between PLS, ethylene signalling, auxin homeostasis and microtubule cytoskeleton dynamics (Chilley *et al.*, 2006). *pls* mutant roots are short, with reduced cell elongation, and they are hyper-responsive to exogenous cytokinins. Expression of the *PLS* gene of *Arabidopsis* is repressed by ethylene and induced by auxin, and influences PIN protein levels in roots (Casson *et al.*, 2002; Chilley *et al.*, 2006; Liu *et al.*, 2013). These and other experimental data reveal that interactions between PLS and PIN is important for the crosstalk between auxin, ethylene and cytokinin (Liu *et al*., 2013).

Mathematical modelling of auxin transport and patterning by constructing multicellular systems in 2-D previously suggested that correct PIN protein placement is necessary to establish correct auxin patterning (Grieneisen *et al*., 2007; Mironova *et al*., 2012). Here we develop a spatiotemporal model of hormonal crosstalk for the *Arabidopsis* root and show that the level and patterning of auxin, PIN localization and *PLS* gene expression in *Arabidopsis* wildtype and mutant roots can be elucidated by the action of spatiotemporal dynamics of hormonal crosstalk, involving the integration of auxin, ethylene and cytokinin signalling and the functioning of the auxin transporters AUX1 and PIN.

## MATERIALS AND METHODS

### Plant materials

Wildtype (Col-0, C24) ecotypes and the *pls* and *pls etr1* mutants of *Arabidopsis thaliana* have been described previously (Topping & Lindsey, 1997; Casson *et al.*, 2002; Chilley *et al*., 2006.). *pls* DR5::GFP seedlings were generated by crossing (Liu *et al*., 2010). For *in vitro* growth studies, seeds were stratified, surface-sterilized and plated on growth medium (half-strength Murashige and

Skoog medium (Sigma, Poole, UK), 1% sucrose, and 2.5% Phytagel (Sigma) at 22 ± 2°C as described (Casson *et al*., 2009).

**Microscopy and image analysis**

Confocal images (for GFP imaging) were taken with a Leica SP5 microscope (Leica Microsystems, Milton Keynes, UK) after counterstaining tissues with 10 mg/ml propidium iodide as described (Casson *et al*., 2009). For image analysis, the mean GUS staining or fluorescence intensity was measured with ImageJ (National Institutes of Health, http://rsb.info.nih.gov/ij <http://rsb.info.nih.gov/ij>). Statistics were carried out using Excel (Microsoft). Results were visualized as average intensities with error bars representing standard deviation of the mean.

**Numerical methods**

The set of partial differential equations, which describes spatiotemporal dynamics of hormonal crosstalk in the root (Figs. 1 and 2), is solved using the finite volume method, in which each grid point is used as an element to establish the discrete mass balance equations. The nonlinearity of the reactive terms for all species in the discrete equations is solved by the Picard iteration, and the resulting linear system equations are solved by the preconditioned conjugate-gradient iterative method. The numerical simulations involve two iterations: one for solving the nonlinearity and the other for solving the linear system of equations. In this work, the convergence tolerance for the iteration of solving nonlinearity and for that of solving the linear systems is $10^{-5}$ and $10^{-10}$, respectively. Much smaller convergence tolerances for both iterations are also tested and the numerical results show that further reduction of convergence tolerances for both iterations does not improve the accuracy of numerical simulations.

**Comparison of experimental data and modelling results**

In this work, experimental images were analysed using ImageJ (http://imagej.nih.gov/ij). The output of ImageJ is the intensity of each pixel in an experimental image. The relative intensity over the whole image shows the relative hormone response or protein concentration patterning for any measured component. The detailed method for using ImageJ to analyse experimental images is described in Methods S1.

In order to implement the numerical simulations, the root (Fig. 1a) was discretised into 2 μm by 2 μm areas, each of which is represented by a grid point. The discrete mass balance equations at each

grid point were established, and the spatiotemporal dynamics of all components (hormones, proteins and mRNAs) were analysed (the method for discretising the root and for implementing numerical simulations is detailed in Methods S2). The outputs of modelling analysis include the concentrations of all components at each grid point; and all reaction rates and transport fluxes. Using the concentration of a component (e.g. auxin) at each model grid point, we calculated firstly the model average of the component over the area described by the root structure (Fig. 1a), which was compared with the experimentally measured level of this component. For example, the average model concentration of auxin in the root was compared with the experimentally determined level of auxin. Secondly, we modelled the concentration patterning of the component, represented by a colour map that shows the concentration at each grid point. We compared this result with the experimental image. Since an experimental image can represent response rather than concentration itself, we noted this difference when making the comparison. The modelling colour map was directly compared with an experimental image, showing the similarities or differences in patterning. For example, an auxin maximum at or close to the QC in a modelling colour map can be compared with an auxin IAA2::GUS response maximum at or close to the QC. If the maximum in modelling output does not emerge or emerges at a different area, the patterning difference between experimental data and modelling results can be identified. Thirdly we modelled the concentration profile of the component. In principle, since the concentration at each individual grid point can be calculated from the model, the concentration average can be calculated for any number of grid points. A useful concentration profile can be generated by calculating a series of cross-sectional averages and using them to plot a concentration profile along the longitudinal root axis. This concentration profile can also be generated for different cell types. Similar relative response or concentration profiles can be generated from experimental images using ImageJ. Therefore, we can compare a modelling concentration profile with an experimental response or concentration profile.

To compare a component between wildtype and mutant roots, we concentrate on trend changes in level, patterning and profile. For example, experimental data show that the auxin level in *pls* is lower than that in the wildtype (Chilley *et al.*, 2006), and the auxin level in *pls etr1* is higher than that in *pls* but lower than that in wildtype (Chilley *et al.*, 2006). As long as modelling results generate the same trend as experimental observations, we considered the modelling result to be similar to or in agreement with experimental measurements.

## RESULTS

### A spatiotemporal model of hormonal crosstalk for *Arabidopsis* root development

Figs. 1 and 2 schematically describe a multicellular hormonal crosstalk model. The model includes 1) a multicellular root structure (Fig. 1a), 2) communication between the multiple root cells (Figs. 1b,c), 3) hormonal crosstalk in each cell (Figs. 1d and 2) and 4) dynamic recycling of the auxin carriers PIN and AUX1 to and from the plasma membrane (Fig. 1e). For simplicity, we do not distinguish between the cell wall and the plasma membrane in this work and individual plasma membrane properties are included in cell wall properties. The equations and parameters used to describe the processes in Figs. 1 and 2 are included in Table S1.

--- Figures 1 and 2 here ---

We set up a 2-D multicellular root structure using previous work as a starting point (Grieneisen *et al*., 2007). Since the lengths of cells in the elongation zone increase proximally (i.e. shootwards from the root meristem, Beemster & Baskin 1998), we have adapted the root structure previously modelled by Grieneisen *et al*. (2007) to include this feature to describe more realistically cell shapes in the *Arabidopsis* root (Fig. 1a). The root structure is defined by a matrix of grid points, each of which has specific properties which define the cytosol or cell wall. Communication between the multiple cells describes how three hormones (auxin, ethylene and cytokinin) and the products of the associated gene expression move in the cytosol, between the cytosol and cell wall, in the cell wall and at the shoot-root boundary (Figs. 1b,c) (Methods S2). Following previous work (Grieneisen *et al*., 2007; Mironova *et al*., 2012), we consider that auxin is moved out of the cell by the PIN transporter system and into the cell by the AUX1 transporter (Methods S2). Moreover, ethylene and cytokinin diffuse freely across the plasma membrane. All other species are assumed to diffuse only within cytosolic space and cannot diffuse across the plasma membrane into the cell wall. At the shoot-root boundary, following previous work (Grieneisen *et al*., 2007), auxin influx from shoot to root occurs only in the pericycle and vascular cell files. This influx into the root is inhibited by downstream ethylene signalling (designated X in our model), based on experimental evidence which indicates that a relatively high ethylene signalling response inhibits the transport of auxin from the shoot to the root tip (Suttle, 1988; Chilley *et al*., 2006) (Methods S2). In addition, auxin efflux from the root towards the shoot occurs only in the epidermal cells (Fig. 1a). This efflux is facilitated by PIN proteins (Methods S2).

Hormonal crosstalk in the cytosol of each cell describes the production and decay of auxin, ethylene and cytokinin and the products of associated gene expression (mRNA and protein; Figs. 1d and 2). The regulatory relationships in Figs.1d and 2 were previously established by iteratively combining experimental measurements with modelling analysis (Liu *et al*. 2010; 2013). In this work, we further consider that AUX1 activities are positively regulated by the downstream ethylene signalling based on experimental observation (Figure 7B in Ruzicka *et al.*, 2007).

Fig. 1e describes the dynamic recycling of PIN and AUX1 protein between the cytosol and plasma membrane. Experimental evidence shows that PIN endocytic internalization is inhibited by auxin (Paciorek *et al*., 2005), and so the model includes auxin inhibition of PIN cycling from the plasma membrane to the cytosol.

**Model fitting reveals that both PIN and AUX1 activities must be restricted to certain ranges in order to generate correct auxin patterning**

The parameters used in this work are included in Table S1. We have used parameter values available in the literature. For example, the diffusion coefficient for auxin is set to 220 $\mu m^2/s$ (Rutschow *et al*., 2011), PIN efflux permeability to 0.5–5 μm/s, with a median value of 2 μm/s (Kramer *et al.*, 2011) and AUX1 influx permeability to1.5 ± 0.3 μm/s (Rutschow *et al*. 2014). It has also been suggested that AUX1 influx must be equal to or greater than PIN efflux otherwise cells would be depleted of auxin (Kramer, 2004). We chose values for these parameters from the above experimental measurements. Parameters relating to ethylene receptor function and CTR1 were studied by Diaz & Alvarez-Buylla (2006), and we used the-parameter rate values from their work. Unknown parameter values were adjusted to produce simulation results consistent with experimental data and images and to meet the following criteria: 1) endogenous average auxin concentration for the WT root is similar to experimental data; 2) the trend changes in average auxin concentration in WT, the *pls* mutant, the *pls etr1* double mutant, and PLS-overexpressing transgenics (PLSox) follow experimental trends (Fig. S1); 3) auxin concentration patterning in the WT root is similar to experimental response patterning (Fig. 3); 4) the auxin carrier proteins PIN and AUX1 localise predominantly to the plasma membrane (Fig. S2); and 5) cytokinin (CK) concentration in the vascular and pericycle cells is higher than that in the epidermal cells (Fig. S3).

Model fitting by manually adjusting unknown parameters reveals that both PIN and AUX1 permeability must be restricted to certain ranges in order to generate the auxin concentration patterning that is similar to experimental IAA2::GUS response patterning. For example, if both PIN and AUX1 permeability is low, the auxin gradient towards the distal region of the root is gradually

smoothed out. If PIN permeability increases, an increase in AUX1 permeability is required to maintain a similar auxin patterning to experimental data (Fig. S4). Although the auxin gradient has been hypothesized to be sink-driven (Friml *et al*., 2002) and computational modelling suggests that auxin efflux carrier permeability may be sufficient to generate the gradient (Grieneisen *et al*., 2007; Wabnik *et al*., 2010), recent work shows that AUX1 is also essential to create the auxin gradient at the root tip (Band *et al*. 2014). Our modelling results support the view that both PIN and AUX1 permeability work together to generate auxin patterning. If AUX1 permeability is not varied in the model such that it becomes a limiting factor for auxin transport, the importance of AUX1 permeability for generating an auxin gradient cannot be revealed. In a previous study, effects of varying AUX1 permeability were not reported (Grieneisen et al., 2007).

Model fitting also reveals that, if cytokinin is allowed to be synthesized in all cells, cytokinin concentration in the epidermal cells is higher than in the vascular and pericycle cells. If we consider that ARR5::GUS signalling reflects cytokinin concentration, then the modelling result is different from experimental measurement. However, if cytokinin biosynthesis occurs predominantly in the vascular and pericycle cells (modelled by limiting synthesis to the vascular and pericycle cells), the modelled cytokinin concentration in the vascular and pericycle cells is higher than that in the epidermal cells, a result similar to experimental observations. Nevertheless, the trend of cytokinin patterning along the longitudinal root axis still differs between the experimental images and modelling results (Fig. S3). These results may indicate that cytokinin biosynthesis is predominantly restricted to the vascular and pericycle cells, by an as yet poorly understood regulatory mechanism, which is supported by experimental evidence indicating that cytokinin biosynthesis may be tissue-specific (Miyawaki *et al*., 2004). The difference in longitudinal cytokinin patterning suggests possible additional unknown regulatory factors which influence patterning along the root axis. In this work, we allow cytokinin biosynthesis to occur only in the vascular and pericycle cells.

An example of model fitting outcomes is shown in Fig. 3 and all other modelling fitting results are included in the SI appendix (Figs. S2, S3, S4). Fig. 3 shows that the modelled auxin concentration patterning in the wildtype *Arabidopsis* root is similar to the experimentally determined auxin IAA2::GUS response patterning, with an auxin maximum established at or close to the QC (Grieneisen *et al*., 2007). The modelled auxin concentration profile is also similar to the auxin IAA2::GUS response profile generated from the Grieneisen *et al*. (2007) experimental image. Moreover, we have analysed auxin concentration profiles for each of the three different types of cell in the model (epidermal, pericycle and vascular) shown in Fig. 1a. Fig. S5 shows that the

concentration profiles for the three cell types follow similar trends to that in Fig. 3. Moreover, an auxin maximum is predominantly established in the central tissues at or close to the QC.

Experiments have shown that the auxin response can be regulated by different effectors, and therefore is not necessarily equivalent to auxin concentration (Vernoux *et al.*, 2011; Cho *et al.*, 2014). Although our modelling results (Figs. 3 and S5) are similar to auxin IAA2::GUS response, we further experimentally measured auxin DII-VENUS response (Fig. S6) and compared it with our modelling results. Fig. S6 shows that in the meristematic zone and QC, the modelled concentration profile is similar to the experimental auxin response profile derived from the DII-VENUS response. However, in the elongation zone, the modelled concentration profile is not in agreement with experimental DII-VENUS imaging. In Notes S1, we further discuss the comparison between modelling results and experimental DII-VENUS response. In particular, we compare our modelling results with experimental observations in the literature (Brunoud *et al*., 2012; Band *et al*., 2014) (Notes S1). Our analysis shows that our modelling results are in reasonably good agreement with experimental data. Specifically, the trend of the modelled auxin levels for 5 cell types (i.e. quiescent centre, stele, endodermis, epidermis meristem and cortex meristem) is similar to the trend observed experimentally (Figure 1K in Band *et al*., 2014). Modelling also shows that the vascular, pericycle and epidermal cells have high, medium and low relative auxin levels, respectively (Notes S1). This trend is in agreement with experimental observations (Fig. 2B in Brunoud *et al*., 2012). In Notes S1, we also discuss the discrepancies between our modelling results and the experimental observations of DII-VENUS response.

Therefore, auxin concentration patterning generated by our model, with an auxin maximum established at or close to the QC, is similar to both experimental IAA2::GUS and DII-VENUS response patterns (Figs. 3 and S6).

---Figure 3 here---

After the model was parameterised following the above model fitting criteria, a wildtype root was defined. We further evaluated model sensitivity (Notes S2), showing that modelling results are robust to variations in parameter values. We then used the model to study the level and patterning of hormones and gene expression in *Arabidopsis* roots.

## Auxin flux from shoot to root and auxin patterning in the *aux1* mutant

Assuming that rootward auxin flux measured in inflorescence stem segments is similar to shoot to root auxin flux at the shoot-root boundary, experimental measurements of the shoot to root auxin flux in inflorescence stem segments for wildtype, *pls* mutant and *pls etr1* double mutant show that auxin flux from shoot to root in the *pls* mutant is significantly lower than that for wildtype. This effect reduces the total amount of auxin in the root tip, and reduces auxin responses in the *pls* root. The auxin flux into the root, and the root auxin content for the *pls etr1* double mutant also recovers approximately to the level of the wildtype (Fig. 4e in Chilley *et al*., 2006). Although the modelled auxin flux into the root for the *pls etr1* double mutant is slightly higher than that for wildtype, our modelling analysis exhibits a similar trend to experimental observation (Fig. 4). Therefore, spatiotemporal dynamics of hormonal crosstalk correctly predicts shoot to root auxin flux in different genotypes.

---Figure 4 here---

Analysis of the experimental images of auxin response patterning in wildtype and the *aux1* mutant shows a decrease in auxin response in the root for *aux1* compared to wildtype (Figs 4a,b), consistent with experimental auxin assays (Swarup *et al*., 2001). By considering that in addition to AUX1, there are other auxin influx carriers (such as LAX proteins) which are not described in the model, we assume that auxin influx permeability in the *aux1* mutant is reduced by 50%. Auxin concentration profiles generated by modelling (Figs. 5c and 5d) are similar to the corresponding experimental auxin response profiles (Figs. 5a and 5b). In both modelled and experimental profiles, the auxin concentration or response maximum for *aux1* is slightly lower than that for wildtype in the QC region, and in both *aux1* and wildtype, auxin concentrations or responses decrease towards the proximal region of the root tip, to reach approximately the same level. Therefore the model for spatiotemporal dynamics of hormonal crosstalk correctly predicts auxin patterning in the *aux1* mutant. This indicates that integration of auxin influx permeability into the hormonal crosstalk is able to explain auxin patterning in specific mutants.

---Figure 5 here ----

## Concentration levels of cytokinin, ethylene and PIN protein

Auxin can negatively regulate cytokinin biosynthesis (Nordstrom *et al*., 2004). The accumulated concentration of cytokinin is described in the hormonal crosstalk network as the balance between its biosynthesis and its removal (Fig. 2). Fig. 6a predicts that, in the *pls* mutant, the average endogenous cytokinin concentration for the root is increased to ca. 1.9-fold of that in wildtype. Experimental measurements show that different cytokinins have significantly different fold changes. However, the general trend is that endogenous cytokinin levels in the *pls* mutant are significantly increased, with a median fold change being 1.42 (Table 1 in Liu *et al*., 2010).

Experimentally it has been shown that *PLS* transcription does not affect ethylene concentration (Chilley *et al*., 2006) and this result is in agreement with our simulations (Fig. 6a). In addition, the relative PIN protein concentration in wildtype, PLSox and *pls, etr1* and *pls etr1* mutants were experimentally measured (Figure 1 in Liu *et al*., 2013). The relative average root concentrations predicted by the model show similar trends to those observed experimentally (Fig. 6b).

In conclusion, modelling predictions for the average levels of cytokinin, ethylene and PIN protein in *Arabidopsis* wildtype and mutant roots are in agreement with experimental observations, suggesting that the levels of hormones and proteins are controlled by the integrative system of hormonal crosstalk (Figs. 1 and 2).

---Figure 6 here---

**PIN patterning in *Arabidopsis* wildtype and mutant roots**

Since it was possible to explain the average PIN protein concentration in different mutants using the spatiotemporal model of hormonal crosstalk (Fig. 6), we went on to ask whether PIN patterning in the *Arabidopsis* root is also controlled by the integrative system of hormonal crosstalk (Figs. 1 and 2). To address this question, we compared experimental evidence for PIN1 and PIN2 patterning with modelling predictions.

The relative concentration data were extracted from experimental images of PIN1 and PIN2 protein localization in wildtype, *pls, etr1* and PLSox seedlings and the *pls etr1* double mutant (Fig. 1a in Liu *et al*., 2013). Data were plotted as PIN concentration profiles for comparison with modelling results.

PIN1 protein is localized in the root mainly in the vascular cells (Blilou *et al*., 2005). PIN1 concentration profiles were generated using the experimental data from the vascular tissues only and compared with the corresponding profiles from the vascular and pericycle cells in the model

(Fig. 1). PIN1 protein predominantly localises to, and is active in, the plasma membrane. A modelled concentration profile based on each grid point tends to mask trend changes due to large variations in PIN1 concentration between the plasma membrane and cytosol. Therefore, to smooth out the concentration differences and more clearly demonstrate PIN1 trends in the model, we calculated the average PIN1 concentration for each cell tier cross-section of the root rather than for cross-sections at each grid point position along the longitudinal root axis. The experimental images (Fig. 1a, Liu *et al*., 2013) approximately represent a region of 5 to 25 cell tiers from the tip. A similar region in modelling outputs is marked by the arrow in Fig. 7b. The trends in Fig. 7a, derived from the experimental images, should be approximately compared with the region marked by the arrow in Fig. 7b. As shown in Fig. 7, the trends of PIN1 patterning in experimental images of wildtype and mutant roots were found to be similar to the corresponding outcomes of modelling simulations, suggesting that PIN1 patterning is due to the action of hormonal crosstalk in wildtype and mutant/PLSox roots.

--- Figure 7 here ---

Modelling analysis further revealed that changes in PIN1 patterning in wildtype and mutant/PLSox roots reflect changes in the *PIN1* transcription rate due to different contributions of auxin, ethylene and cytokinin. For example, modelled PIN1 patterning in wildtype shows that PIN1 levels generally decrease from the proximal region to the distal region of the root (Fig. 7a). However, in the *pls* mutant, an opposite trend emerges (Fig. 7a). Model calculation shows that, in the *pls* mutant, the *PIN1* transcription rate has significantly increased at the region near the root tip (Fig. S7). Further modelling analysis reveals that, in the wildtype, the downstream component of ethylene signalling, designated X, is suppressed due to the action of PLS at the region near the tip (Fig. S8). PLS patterning displays an increasing abundance from the proximal to the distal end of the root, due predominantly to the regulation of *PLS* expression by auxin (Fig. S8; also see "**Modelling prediction on the patterning of *POLARIS* (*PLS*) expression pattern is confirmed by experiments"** section). In the *pls* mutant, the suppression of X is relaxed due to the loss of PLS function. This enhances the rate of PIN1 biosynthesis at the region near the tip and therefore PIN1 patterning shows an increasing concentration trend from the proximal to the distal region. In addition, in the *pls* mutant, the auxin concentration decreases (Fig. S1) and the cytokinin concentration increases (Fig. 6). As auxin positively regulates and cytokinin negatively regulates *PIN1* transcription, the increase in *PIN1* transcription rate at the region near the tip also reflects the effects of both auxin and cytokinin signalling.

Therefore, the overall effects of auxin, ethylene and cytokinin result in opposite trends in PIN1 patterning in wildtype and *pls* mutant roots. This example demonstrates that spatiotemporal hormonal crosstalk, which describes simultaneous actions of multiple hormones and the associated genes, is necessary for specifying the patterning of PIN1 in the root. Fig. 7 further shows that the modelled patterning trend of PIN1 for wildtype, *pls*, *etr1* and PLSox (the region is denoted by the arrow) is similar to the corresponding experimental trend. However, a noticeable difference for *pls etr1* double mutant can be identified. This indicates the limitation of our model for analysing this double mutant.

Patterning of PIN2 protein was also analysed (Fig. S9). Modelling predictions on the patterning of PIN2 protein for wildtype and PLSox are in reasonable agreement with experimental data. However, discrepancies between modelling results and experimental data emerge for other mutants. In Fig. S9, we further describe and discuss these results.

**Modelling prediction of *POLARIS* expression pattern is confirmed by experiments**

As shown in Fig. 2, the *PLS* gene of *Arabidopsis*, which transcribes a short mRNA encoding a 36-amino acid peptide (Casson *et al*., 2002; Chilley *et al*., 2006), is important for establishing crosstalk between auxin, ethylene, and cytokinin. Here we used both experimental analysis and modelling to investigate further the control of the patterning of *PLS* gene expression.

--- Figure 8 here ---

Experimental imaging of PLS protein accumulation in wildtype root (Fig. 8a) shows a concentration maximum near the distal region, with the concentration declining towards the proximal region of the root. This is similar to the expression of the *PLS* gene as monitored by *PLS* promoter-GUS analysis (Casson *et al*., 2002, Chilley *et al*., 2006). PLS concentration profile generated from the experimental fluorescence image (Fig. 8a) graphically illustrates this patterning (Fig. 8b). The spatiotemporal modelling of hormonal crosstalk predicts the same trend (Fig. 8c), indicating that the hormonal crosstalk network (Fig. 2) controls the patterning of *PLS* gene expression and protein accumulation. Modelling calculations reveal that the rate of *PLS* transcription reaches a maximum in the distal part of the root (Fig. S10), resulting in the patterning of *PLS* expression (Fig. 8). As indicated in Fig. 8d, if *PLS* transcription is not regulated by auxin, the modelled patterning of *PLS* expression is not in agreement with experimental observation. This reflects the predominant role of auxin in the regulation of *PLS* expression .

**Ethylene and AUX1 patterning in *Arabidopsis* wildtype root**

Modelling prediction of the endogenous ethylene concentration patterning is similar to experimentally determined response patterning (Martin-Rejano *et al*., 2011). Both modelling and experimental results show increases in ethylene responses towards the proximal part of the root (Fig. S11).

In this work, we consider that AUX1 activity is positively regulated by the downstream ethylene signalling based on experimental observation (Figure 7B in Ruzicka *et al.*, 2007). Model results for AUX1 patterning (Fig. S12) are in part similar to experimental imaging (Fig. S8 in Band *et al.* 2014) with AUX1 levels increasing proximally in the epidermis, and higher AUX1 levels in the outer cell layers compared to the central cell cylinder. Experimentally, it has been shown that, within the epidermis, AUX1 is present mainly in the elongation zone cells (Band *et al.* 2014). However, the model does not exhibit the elevated experimental AUX1 levels in the columella and near the QC or the proximally declining AUX1 levels in the central cylinder. The differences between modelling and experimental results may indicate that, in addition to ethylene, other effectors may also regulate AUX1 activity.

## DISCUSSION

Experimental information accumulated over many years indicates that, in root development, hormones and the associated regulatory and target genes form a network in which relevant genes regulate hormone activities and hormones regulate gene expression. Functionally important patterns of hormone distribution, hormone responses and gene expression are presumed to emerge from these interactions. However, little is known about how this patterning is generated. By developing an integrative model that combines experimental data, the construction of a hormonal crosstalk network, a spatial root structure for cell-cell interactions and spatiotemporal modelling, we demonstrate that the spatiotemporal dynamics of hormonal crosstalk establishes the causal relationship for the level of auxin, ethylene, cytokinin, PIN protein and PLS protein, as well as the mechanisms for generating patterning in these hormones and proteins.

In this work, we set up a 2-D multicellular root structure using previous work as a starting point (Grieneisen *et al*., 2007). Although the root structure described by Fig. 1a is a representative description of *Arabidopsis* root, it is incomplete and lacks a lateral root cap. Future research could therefore include additional features to understand for example how a lateral root cap contributes to the spatiotemporal dynamics of hormonal crosstalk, and how the spatiotemporal dynamics of

hormonal crosstalk is formed in a 3-D multicellular root structure with the sub-cellular resolution. Experiments have shown that a lateral root cap is important for transporting auxin from the apical area to elongation zone (Swarup *et al*., 2005; Band *et al*., 2014).

The work presented in this paper provides a framework for studying the level and patterning of hormone distribution, hormone responses and gene expression by iteratively combining experimental data with the construction of a hormonal crosstalk network, a spatial root structure for cell-cell interactions, and spatiotemporal modelling. We show that the level and patterning of auxin, ethylene and cytokinin responses, and expression of *PIN*s and *PLS* can be explained by spatiotemporal hormonal crosstalk in the *Arabidopsis* root, as summarised in Fig. 9.

--- Figure 9 here---

Experimental analysis has shown that PIN levels in *Arabidopsis* vary in response to a range of hormones. Auxin positively regulates levels of several PIN proteins in different developmental contexts (Blilou *et al*., 2005; Laskowski *et al*., 2006; Chapman & Estelle, 2009; Vanneste & Friml, 2009) by a signalling pathway regulating transcription (Woodward & Bartel, 2005), and also by promoting accumulation at the plasma membrane (Paciorek *et al*., 2005). Ethylene also upregulates *PIN*s (e.g. *PIN2*, Ruzicka *et al*., 2007) while cytokinin negatively regulates *PIN1, PIN2 and PIN3* (Ruzicka *et al*., 2009; Bishopp *et al*., 2011a), but positively regulates *PIN7*. In this work, we concentrate on the investigation of PIN1 and PIN2. In addition, as PIN3, which is negatively regulated by cytokinin, and PIN7, which is positively regulated by cytokinin, are localised at similar positions (Ruzicka *et al*., 2009; Bishopp *et al*., 2011a) in the root, it may be reasonable to assume that the overall effects of cytokinin on both PIN3 and PIN7 lead to little net effect on auxin transport. PIN levels are also influenced by other genes. For example, in the *pls* mutant, both PIN1 and PIN2 levels increase (Liu *et al*. 2013). It is also evident that ethylene activates the biosynthesis of auxin locally in the root tip (Stepanova *et al*., 2007; Swarup *et al*., 2007), and that both auxin and cytokinin can synergistically activate the biosynthesis of ethylene (Chilley *et al*., 2006; Stepanova *et al*., 2007). Numerous experimental analyses have shown that auxin patterning, with a localized concentration maximum in the root tip, is pivotal for correct root development (Sabatini *et al*., 1999), and that hormonal interactions determine PIN localization patterns (Liu *et al*., 2013).

During *Arabidopsis* root development, both the level and patterning of proteins are interlinked. In the wildtype root, PIN1 levels generally decrease from the proximal to the distal region (Fig. 7) and PLS levels generally increase from the proximal end to the distal end (Fig. 8). However, in the *pls*

mutant, PIN1 levels generally increase from the proximal end to the distal end. In addition, in the *pls* mutant, the average auxin, ethylene and cytokinin concentration or response in the root is reduced, remains approximately constant, and is increased respectively (Chilley *et al*., 2006; Liu *et al*., 2010) while the average PIN1 level increases (Liu *et al*., 2013). This work shows that the causal relationship between the level and patterning of PIN1 and PLS proteins can be established by studying the spatiotemporal dynamics of hormonal crosstalk.

In order for the root to generate auxin patterning similar to experimental results, the permeability of both the PIN and AUX1 auxin carrier proteins is important, and must be limited to certain ranges. It can be concluded that both PIN and AUX1 proteins work together to generate auxin patterning similar to experimental results. It has been suggested that AUX1 influx must be at least equal to PIN efflux to avoid auxin depletion in the cells (Kramer *et al*., 2004). Previous modelling work has separately suggested that both the auxin efflux carrier PIN activity (Grieneisen *et al*., 2007; Wabnik *et al*., 2010) and AUX1 activity (Band *et al*., 2014) are essential to create the auxin gradient at the root tip. Our results suggest that, due to the action of a hormonal crosstalk network, the coordination of AUX1 and PIN activity is related to many aspects of PIN and AUX1 proteins, including transcription, translation, decay, and recycling of the AUX1 to PIN proteins between the plasma membrane and intracellular compartments.

The discrepancy between experimental and modelling results for cytokinin patterning suggests that unknown molecular mechanisms exist for regulating cytokinin biosynthesis and/or degradation, and further experimental investigations are required to elucidate these mechanisms. The rate limiting step for cytokinin biosynthesis involves a group of isopentenyltransferase (IPT) enzymes. While *IPT* genes are expressed throughout the root, different genes appear to display tissue specific expression at different levels. In the root, *IPT* genes are predominantly expressed in the xylem precursor cells, the phloem tissue, the columella, and the endodermis of the elongation zone (Miyawaki et al., 2004). This expression patterning appears to be supported by ARR5::GUS cytokinin response imaging (Fig. S3). In this image, ARR5::GUS cytokinin response in the epidermal and cortical cells is much lower than that in the central cells. Experimental evidence therefore indicates that cytokinin biosynthesis may be tissue-specific. In our model, cytokinin biosynthesis was restricted to the central pericycle/border, vascular and columella cells.

Our modelling results for cytokinin concentration patterning (Fig. S3) are quantitatively different from experimental observations (revealed as *ARR5::GUS* expression, as a proxy for cytokinin distribution; Werner *et al*., 2003). The modelled cytokinin concentration increases from the distal to

the proximal region of the root. This patterning is consistent with the reduction of auxin concentration/response from the distal to the proximal region, as described in our hormonal crosstalk network (Fig. 2) where auxin negatively regulates cytokinin biosynthesis based on experimental observations (Nordstrom *et al*., 2004). However, this cytokinin patterning is opposite to the data based on experimental images (Werner *et al*., 2003).

This discrepancy leads to the following possibilities. First, the experimental data (Nordstrom *et al*., 2004) show that the auxin-mediated regulation of cytokinin biosynthesis is different for iP and Z types. While biosynthesis of the Z type is inhibited by auxin, the iP type may not be inhibited by auxin. Thus, a detailed description of the regulatory relationship between auxin concentration and cytokinin biosynthesis for root development requires experimental measurement to determine the location of specific types of cytokinin in the root, and then to derive how cytokinin biosynthesis and degradation are regulated at each location. Second, the cytokinin patterning derived from *ARR5::GUS* images (Werner *et al*., 2003) may not accurately represent the patterning of cytokinin concentration and therefore may not be directly comparable to modelled patterning of cytokinin concentration. The *ARR5::GUS* images measure the activation of the *ARR5* promoter by cytokinin, therefore indicating the activity of cytokinin signalling rather than cytokinin concentration. Bishopp *et al*. (2011a) have discussed that AHP6, which inhibits the cytokinin signalling pathway and *ARR5* expression, is regulated by auxin in the xylem axis. This may indicate that *ARR5::GUS* images represent the effects of both cytokinin and AHP6 concentration, and therefore may not solely reflect cytokinin concentration. Third, it has been demonstrated that cytokinin is transported from the shoot to root in the phloem (Bishopp *et al*., 2011b) which, in combination with local biosynthesis, degradation and diffusion could influence cytokinin concentration and signal patterning in the root tip. Interestingly, in a different context for root development analysis, it has also been shown that an additional component is required to position cytokinin signal patterning (Muraro *et al*., 2014). Therefore, the combination of our analysis in this work with the information in the literature indicates that the patterning of cytokinin concentration and signalling requires further experimental and modelling studies.

Based on experimental results (Nordstrom *et al*., 2004), our hormonal crosstalk network (Fig. 2, Liu *et al*., 2013) describes a negative regulation of auxin biosynthesis by cytokinin. However, Jones *et al*. (2010) have shown that cytokinin positively regulates auxin biosynthesis in young developing tissues (10 DAG). In previous work, our hormonal crosstalk network analysis has revealed that both sets of experimental results (Nordstrom *et al*., 2004; Jones *et al*., 2010) can be incorporated into the hormonal crosstalk network, leading to the same conclusions about other regulatory relationships of

hormonal crosstalk (Liu *et al*., 2013). In the current research, we have analysed both cases using the same spatial setting (Fig. 1) and our modelling results indicate that each leads to qualitatively similar results. Therefore, the conclusions we have drawn in this work are applicable to both cases. In the current paper, we have concentrated on an analysis based on the experimental results of Nordstrom *et al*. (2004).

In root development, the complexity of hormonal signalling includes many aspects. This work has shown that the spatiotemporal dynamics of hormonal crosstalk, which integrates hormonal crosstalk at a cellular level with root structure, are able to explain two important aspects – the steady-state level and the patterning of hormones/hormone responses and gene expression. Recent studies have shown that growth and hormonal patterning can affect each other (De Rybel *et al*., 2014; Mahonen et al., 2014). Future research should investigate the spatiotemporal dynamics of hormonal crosstalk in the presence of, or in response to, growth.

All recent modelling and experimental work (Chickarmane *et al*., 2010; Bargmann *et al*., 2013; Hill *et al*., 2013; De Rybel *et al*., 2014) shows that integration of regulatory networks into spatial root structures is a promising tool for elucidating mechanisms of development. By integrating other genes into the hormonal crosstalk network (Mintz-Oron *et al*., 2012; Bargmann *et al*., 2013; Hill *et al*., 2013; De Rybel *et al*., 2014.) and by expanding root structure to include more details of cell to cell communication (Chickarmane *et al*., 2010; Hill e*t al*., 2013; De Rybel *et al*., 2014), we should be able to elucidate the level and patterning of other hormones and gene expression in the future.

## ACKNOWLEDGEMENTS

JL and KL gratefully acknowledge Research Councils UK and the Biotechnology & Biological Sciences Research Council (BBSRC) for funding in support of this study; AM and JR are in receipt of BBSRC studentships.

## CONFLICT OF INTEREST

The authors declare that they have no conflict of interest.

## REFERENCES

**Aida M, Beis D, Heidstra R, Willemsen V, Blilou I, Galinha C, Nussaume L, Noh YS, Amasino R, Scheres B. 2004.** The *PLETHORA* genes mediate patterning of the Arabidopsis root stem cell niche. *Cell* **119**: 109-120.

**Band LR, Wells DM, Fozard JA, Ghetiu T, French AP, Pound MP, Wilson MH, Yu L, Li W, Hijazi HI et al. 2014.** Systems analysis of auxin transport in the Arabidopsis root apex. *The Plant Cell* **26**: 862–875.

**Bargmann BO, Vanneste S, Krouk G, Nawy T, Efroni I, Shani E, Choe G, Friml J, Bergmann DC, Estelle M, Birnbaum KD. 2013.** A map of cell type-specific auxin responses. *Molecular Systems Biology* **9**: 688.

**Beemster GTS, Baskin IS. 1998.** Analysis of cell division and elongation underlying the developmental acceleration of root growth in Arabidopsis thaliana. *Plant Physiology* **116**: 1515–1526.

**Bishopp A, Help H, El-Showk S, Weijers D, Scheres B, Friml J, Benkova E, Mahonen AP, Helariutta Y. 2011a**. A mutually inhibitory interaction between auxin and cytokinin specifies vascular pattern in roots. *Current Biology* **21**: 917–926.

**Bishopp A, Lehesranta S, Vaten V, Help H, El-Showk E, Scheres B, Helariutta K, Mahonen AP, Sakakibara H, Helariutta Y. 2011b.** Phloem-transported cytokinin regulates polar auxin transport and maintains vascular pattern in the root meristem. *Current Biology* **21**: 927–932.

**Blilou I, Xu1 J, Wildwater M, WillemsenV, Paponov I, Friml J, Heidstra1 R, Aida M, Palme K, Scheres B. 2005.** The PIN auxin efflux facilitator network controls growth and patterning in Arabidopsis roots. *Nature* **433**: 39–44.

**Brunoud G, Wells DM, Oliva M, Larrieu A, Mirabet V, Burrow AH, Beeckman T, Kepinski S, Traas J, Bennett MJ, Vernoux T. 2012.** A novel sensor to map auxin response and distribution at high spatio-temporal resolution. *Nature* **482**: 103–106.

**Casson SA, Chilley PM, Topping JF, Evans IM, Souter MA, Lindsey K. 2002.** The *POLARIS* gene of Arabidopsis encodes a predicted peptide required for correct root growth and leaf vascular patterning. *The Plant Cell* **14**: 1705–1721.

**Casson SA, Topping JF, Lindsey K. 2009.** MERISTEM-DEFECTIVE, an RS domain protein, is required for meristem patterning and function in Arabidopsis. *The Plant Journal* **57**: 857–869.

**Chandler JW. 2009.** Auxin as compère in plant hormone crosstalk. *Planta* **231**: 1–12.

**Chapman EJ, Estelle M. 2009.** Mechanism of auxin-regulated gene expression in plants. *Annual Review of Genetics* **43**: 265–285.

**Chickarmane V, Roeder A. H, Tarr P. T, Cunha A, Tobin C, Meyerowitz EM.2010.** Computational morphodynamics: a modeling framework to understand plant growth. *Annual Review of Plant Biology* **61**: 65–87.

**Chilley PM, Casson SA, Tarkowski P, Hawkins N, Wang KL, Hussey PJ, Beale M, Ecker JR, Sandberg GK, Lindsey K**. **2006.** The POLARIS peptide of Arabidopsis regulates auxin transport and root growth via effects on ethylene signaling. *The Plant Cell* **18**: 3058–3072.

**Cho H, Ryu H, Rho S, Hill K, Smith S, Audenaert D, Park J, Han S, Beeckman T, Bennett MJ et al.** 2014. A secreted peptide acts on BIN2-mediated phosphorylation of ARFs to potentiate auxin response during lateral root development. *Nature Cell Biology* **16:** 66–76.

**Clark NM, de Luis Balaguer MA, Sozzani R. 2014.** Experimental data and computational modeling link auxin gradient and development in the Arabidopsis root. *Frontiers in Plant Science* **5**: 328.

**De Rybel B, Adibi M, Breda AS, Wendrich JR, Smit ME, Novák O, Yamaguchi N, Yoshida S, Van Isterdael G et al. 2014.** Integration of growth and patterning during vascular tissue formation in Arabidopsis. *Science* **345**: 1255215.

**Del Bianco M, Giustini L, Sabatini S. 2013.** Spatiotemporal changes in the role of cytokinin during root development. *New Phytologist* **199**: 324-338.

**Depuydt S, Hardtke CS. 2011.** Hormone signalling crosstalk in plant growth regulation. *Current Biology* **21**: R365-R373.

**Diaz J, Alvarez-Buylla E. 2006.** A model of the ethylene signalling pathway and its gene response in Arabidopsis thaliana: pathway cross-talk and noise-filtering properties. *Chaos* **16**: 023112, 01–16.

**Eklof S, Åstot C, Blackwell J, Moritz T, Olsson O, Sandberg G. 1997.** Auxin–cytokinin interactions in transgenic tobacco. *Plant and Cell Physiology* **38**: 225–235.

**Friml J, Benkova E, Blilou I, Wisniewska J, Hamann T, Ljung K, Woody S, Sandberg G, Scheres B, Jürgens G, Palme K.** 2002. AtPIN4 mediates sink-driven auxin gradients and root patterning in Arabidopsis. *Cell* **108**: 661–673.

**Grieneisen VA, Xu J, Marée AFM, Hogeweg P, Scheres B. 2007.** Auxin transport is sufficient to generate a maximum and gradient guiding root growth. *Nature* **449**: 1008–1013.

**Hill K, Porco S, Lobet G, Zappala S, Mooney S, Draye X, Bennett MJ. 2013.** Root systems biology: integrative modeling across scales, from gene regulatory networks to the rhizosphere. *Plant Physiology* **163**: 1487–1503.

**Ikeda Y, Men S, Fischer U, Stepanova AN, Alonso JM, Ljung K, Grebe M. 2009.** Local auxin biosynthesis modulates gradient directed planar polarity in Arabidopsis. *Nature Cell Biology* **11**: 731-738.

**Jones AR, Kramer EM, Knox K, Swarup R, Bennett MJ, Lazarus CM, Leyser HMO, Grierson CS. 2008.** Auxin transport through non-hair cells sustains root-hair development. *Nature Cell Biology* **11**: 78–84.

**Jones B, Gunneras SA, Petersson SV, Tarkowski P, Graham N, May S, Dolezal K, Sandberg G, Ljung K. 2010.** Cytokinin regulation of auxin synthesis in arabidopsis involves a homeostatic feedback loop regulated via auxin and cytokinin signal transduction. *The Plant Cell* **22**: 2956–2969.

**Kramer EM. 2004.** PIN and AUX/LAX proteins: their role in auxin accumulation. *Trends in Plant Science* **9**: 578–582.

**Kramer EM, Rutschow HL, Mabie SS. 2011.** AuxV: A databaseof auxin transport velocities. *Trends in Plant Science* **16**: 461–463.

**Krupinski P, Jonsson H. 2010.** Modeling Auxin-regulated Development. *Cold Spring Harbor Perspectives in Biology* **2**: a001560.

**Laskowski M, Biller S, Stanley K, Kajstura T, Prusty R. 2006.** Expression profiling of auxin-treated Arabidopsis roots: toward a molecular analysis of lateral root emergence. *Plant and Cell Physiology* **47**: 788–792.

**Liu JL, Mehdi S, Topping J, Tarkowski P, Lindsey K. 2010.** Modelling and experimental analysis of hormonal crosstalk in Arabidopsis. *Molecular Systems Biology* **6**: 373.

**Liu JL, Mehdi S, Topping J, Friml J, Lindsey K**. **2013.** Interaction of PLS and PIN and hormonal crosstalk in Arabidopsis root development. *Frontiers in Plant Science* **4**: 75.

**Liu J, Rowe J, Lindsey K. 2014.** Hormonal crosstalk for root development: a combined experimental and modeling perspective. *Frontiers in Plant Science* **5**:116.

**Mahonen AP, ten Tusscher K, Siligato R, Smetana O, Díaz-Trivino S, Salojarvi J, Wachsman G, Prasad K, Heidstra R, Scheres B.** 2014. PLETHORA gradient formation mechanism separates auxin responses. *Nature* **515**: 125–129.

**Martin-Rejano EM, Camacho-Cristoval JJ, Herrera-Rodriguez MB, Rexach J, Navarro-Gochicoa MT, Gonzales-Fontes A**. **2011.** Auxin and ethylene are involved in the responses of root system architecture to low boron supply in Arabidopsis. *Physiologia Plantarum* **142**: 170-178.

**Mintz-Oron S, Meir S, Malitsky S, Ruppin E, Aharoni A, Shlomi T. 2012.** Reconstruction of Arabidopsis metabolic network models accounting for subcellular compartmentalization and tissue specificity. *Proceedings of the National Academy of Sciences, USA* **109**: 339–344.

**Mironova VV, Omelyanchuk NA, Novoselova ES, Doroshkov AV, Kazantsev FV, Kochetov AV, Kolchanov NA, Mjolsness E, Likhoshvai VA**. **2012.** Combined in silico/in vivo analysis of mechanisms providing for root apical meristem self-organization and maintenance. *Annals of Botany* **110**: 349–360.

**Mironova VV Omelyanchuk NA, Yosiphon G, Fadeev SI, Kolchanov NA, Mjolsness E, Likhoshvai VA**. **2010.** A plausible mechanism for auxin patterning along the developing root. *BMC Systems Biology* **4**: 98.

**Miyawaki K, Matsumoto-Kitano M, Kakimoto K**. **2004.** Expression of cytokinin biosynthetic isopentenyltransferase genes in Arabidopsis: tissue specificity and regulation by auxin, cytokinin, and nitrate. *The Plant Journal* **37**: 128–138.

**Muraro D, Mellor N, Pound MP, Help H, Lucas M, Chopard J, Byrne HM, Godin C, Hodgman TC, King JR, et al. 2014.** Integration of hormonal signaling networks and mobile microRNAs is required for vascular patterning in Arabidopsis roots. *Proceedings of the National Academy of Sciences, USA* **111**: 857–862.

**Nordstrom A, Tarkowski P, Tarkowska D, Norbaek R, Åstot C, Dolezal K, Sandberg G. 2004.** Auxin regulation of cytokinin biosynthesis in Arabidopsis thaliana: a factor of potential importance for auxin–cytokinin-regulated development. *Proceedings of the National Academy of Sciences, USA* **101**: 8039–8044.

**O' blnqdj S+Y` ylł ` lnu` D+Qt sg` qc s M+Odsq`´sek J, Stierhof Y-D, Kleine-Vehn J. Morris DA, Emans N, Jürgens G, Geldner N, Friml J. 2005.** Auxin inhibits endocytosis and promotes its own efflux from cells. *Nature* **435**: 1251–1256.

**Petrásek J, Petrášek J, Mravec J, Bouchard R, Blakeslee JJ, Abas M, Seifertová D, Wiśniewska J, Tadele Z, Kubeš M, et al. 2006.** PIN proteins perform a rate-limiting function in cellular auxin efflux. *Science* **312**: 914–918.

**Rutschow HL, Baskin TI, Kramer EM. 2011.** Regulation of solute flux through plasmodesmata in the root meristem. *Plant Physiology* **155**:1817-1826.

**Rutschow HL, Baskin TI, Kramer EM. 2014.** The carrier AUXIN RESISTANT (AUX1) dominates auxin flux into Arabidopsis protoplasts. *New Phytologist* **204**: 536-544.

**Ruzicka K, Ljung K, Vanneste S, Podhorska R, Beeckman T, Friml J, Benkova E. 2007.** Ethylene regulates root growth through effects on auxin biosynthesis and transport-dependent auxin distribution. *The Plant Cell* **19**: 2197–2212.

**Ruzicka K, Simásková M, Duclercq J, Petrásek J, Zazímalová E, Simon S, Friml J, Van Montagu MC, Benková E. 2009.** Cytokinin regulates root meristem activity via modulation of the polar auxin transport. *Proceedings of the National Academy of Sciences, USA* **106**: 4284–4289.

**Sabatini S, Sabatini S, Beis D, Wolkenfelt H, Murfett J, Guilfoyle T, Malamy J, Benfey P, Leyser O, Bechtold N, et al. 1999.** An auxin-dependent distal organizer of pattern and polarity in the *Arabidopsis* root. *Cell* **99**: 463-472.

**Sarkar AK, Luijten M, Miyashima S, Lenhard M, Hashimoto T, Nakkajima K, Scheres B, Heidstra R, Laux T. 2007.** Conserved factors regulate signalling in *Arabidopsis thaliana* shoot and root stem cell organizers. *Nature* **446**: 811-814.

**Shi Y, Tian S, Hou L, Huang X, Zhang X, Guo H, Yanga S. 2012.** ethylene signaling negatively regulates freezing tolerance by repressing expression of CBF and type-A ARR genes in Arabidopsis. *The Plant Cell* **24**: 2578–2595

**Stepanova AN, Jun J, Likhacheva AV, Alonso JM. 2007.** Multilevel interactions between ethylene and auxin in Arabidopsis roots. *The Plant Cell* **19**: 2169–2185.

**Suttle JC. 1988.** Effect of ethylene treatment on polar IAA transport, net IAA uptake and specific binding of N-1-naphthylphthalamicacid in tissues and microsomes isolated from etiolated pea epicotyls. *Plant Physiology* **88**: 795–799.

**Swarup K, Benková E, Swarup R, Casimiro I, Péret B, Yang Y, Parry G, Nielsen E, De Smet I, Vanneste S, et al. 2008.** The auxin influx carrier LAX3 promotes lateral root emergence. *Nature Cell Biology* **10**: 946-954.

**Swarup R, Friml J, Marchant A, Ljung K, Sandberg G, Palme K, & Bennett MJ. 2001.** Localization of the auxin permease AUX1 suggests two functionally distinct hormone transport pathways operate in the Arabidopsis root apex. *Genes and Development* **15**: 2648–2653

**Swarup R, Kramer EM, Perry P, Knox K, Leyser HM, Haseloff J, Beemster GT, Bhalerao R & Bennett MJ. 2005.** Root gravitropism requires lateral root cap and epidermal cells for transport and response to a mobile auxin signal. *Nature Cell Biology* **7**: 1057-1065.

**Swarup R, Perry P, Hagenbeek D, Van Der Straeten D, Beemster GT, Sandberg G, Bhalerao R, Ljung K & Bennett MJ. 2007.** Ethylene upregulates auxin biosynthesis in Arabidopsis seedlings to enhance inhibition of root cell elongation. *The Plant Cell* **19**: 2186–2196.

**Tivendale ND, Ross JJ, Cohen JD. 2014.** The shifting paradigms of auxin biosynthesis. *Trends in Plant Science* **19**: 44-51.

**To JP, Haberer G, Ferreira FJ, Deruere J, Mason MG, Schaller GE, Alonso JM, Ecker JR, Kieber JJ. 2004.** Type-A Arabidopsis response regulators are partially redundant negative regulators of cytokinin signaling. *The Plant Cell* **16**: 658–671.

**Topping JF, Lindsey K. 1997.** Promoter trap markers differentiate structural and positional components of polar development in Arabidopsis. *The Plant Cell* **9**: 1713–1725.

**Vanneste S, Friml J. 2009.** Auxin: A trigger for change in plant development. *Cell* **136**: 1005-1016.

**Vanstraelen M, Benkova E. 2012.** Hormonal interactions in the regulation of plant development. *Annual Review of Cell and Developmental Biology* **28**: 463–487.

**Vernoux T, Brunoud G, Farcot E, Morin V, Van den Daele H, Legrand J, Oliva M, Das P, Larrieu A, Wells D, Guedon Y, Armitage L, Picard F, Guyomarc'h S, Cellier C, Parry G, Koumproglou R, Doonan JH, Estelle M, Godin C, Kepinski S, Bennett M, De Veylder L, Traas J. 2011.** The auxin signalling network translates dynamic input into robust patterning at the shoot apex. *Mol Systems Biol* **7:** 508

**Wabnik K, Kleine-Vehn J, Balla J, Sauer M, Naramoto S, Reinöhl V, Merks RMH, Govaerts W, Friml J. 2010.** Emergence of tissue polarization from synergy of intracellular and extracellular auxin signaling. *Molecular Systems Biology* **6**: 447.

**Werner T, Motyka V, Laucou V, Smets R. van Onckelen H, Schmülling T. 2003.** Cytokinin-deficient transgenic Arabidopsis plants show multiple developmental alterations indicating opposite functions of cytokinins in the regulation of shoot and root meristem activity. *The Plant Cell* **15**: 2532–2550.

**Weyers DBW, Paeterson NW. 2001.** Plant hormones and the control of physiological processes. *New Phytolologist* **152**: 375-407.

**Woodward AW, Bartel B. 2005.** Auxin: regulation, action, and interaction. *Annals of Botany* **95**: 707–735.

**Zhao Y**. **2010.** Auxin biosynthesis and its role in plant development. *Annual Review of Plant Biology* **61**: 49–64.

**Fig. S1** Trend in average root auxin concentration in wild type and mutants.

**Fig. S2** Modelling results show that PIN and AUX1 auxin carrier proteins localise predominantly to the plasma membrane in the wild type.

**Fig. S3** Cytokinin images and concentration profiles.

**Fig. S4** Auxin patterning for different combinations of PIN and AUX1 permeability.

**Fig. S5** Modelled auxin concentration profiles for the three different cell types (epidermal, pericycle and vascular cells).

**Fig. S6** DII-VENUS response profile measured from the experimental image, compared to the model auxin concentration profile for wild type root.

**Fig. S7** Modelling results for PINm transcription rates in wild type.

**Fig. S8** Modelling results for patterning of X, downstream of ethylene signalling, and PLSp, POLARIS protein, in wild type.

**Fig. S9** Comparison of experimental and modelling PIN2 patterning for wild type and mutants.

**Fig. S10** Modelling results for PLSm transcription patterning in wild type.

**Fig. S11** Modelling prediction of ethylene patterning is similar to experimental measurements.

**Fig. S12** Modelled AUX1 concentration profiles for the three different cell types (epidermal, pericycle and vascular cells).

**Table S1** Model equations and parameter values for the model described in Figures 1 and 2.

**Methods S1** Using ImageJ to analyse experimental images.

**Methods S2** Method for discretising the root and for implementing numerical simulations.

**Notes S1** Comparison of modelled auxin concentration trend with experimental DII-VENUS data in the literature.

**Notes S2** Evaluation of model sensitivity.

## Figure Legends

Figure 1. A schematic description of the model that describes 2-D root structure, cell-cell communication and the hormonal crosstalk network in each cell. a: Multicellular root structure (adapted from Grieneisen *et al*. 2007) defined by a matrix of grid points (GP) which form the root map. MZ – meristematic zone. EZ – elongation zone. b: Auxin flux by permeability from shoot to root in the pericycle and vascular cell files and from root to shoot in the epidermal files. ET and CK flux by diffusion between shoot and root. c: Species flux between nearest neighbour GP by diffusion within the cytosol (all species) or cell wall (hormones) and hormone flux across the plasma membrane by diffusion (ET and CK) and permeability (auxin). d: The hormonal crosstalk network in each cell (Figure 2). e: Dynamic recycling of the auxin carriers PIN and AUX1 by exocytosis and endocytosis to and from the plasma membrane. Auxin inhibits endocytosis of the PIN proteins (Paciorek *et al*., 2005).

Figure 2. The hormonal crosstalk network in each cell. The network is constructed by adding AUX1 biosynthesis module to the hormonal crosstalk network we previously developed (Liu *et al*. 2010, 2013). **Symbols**: Auxin: Auxin hormone, ET: ethylene, CK: Cytokinin, PINm: PIN mRNA, PINp: PIN protein, PLSm: POLARIS mRNA, PLSp: POLARIS protein, X: Downstream ethylene signalling, Ra*: Active form of auxin receptor, Ra: Inactive form of auxin receptor, Re*: Active form of ethylene receptor, ETR1. Re: Inactive form of ethylene receptor, ETR1, CTR1*: Active form of CTR1, CTR1: Inactive form of CTR1, AUX1 m: AUX1 mRNA, AUX1 p: AUX1 protein.

Figure 3. Auxin concentration patterning in the wildtype Arabidopsis root is similar to experimental observation. a: Experimental image (Grieneisen *et al*., 2007) and response profile analysed using Image J. b: Model concentration colour map and profile (colour bar units: μM).

Figure 4. Modelling prediction of auxin flux from shoot to root is similar to experimental measurements (Fig. 4e from Chilley *et al*., 2006. www.plantcell.org, Copyright American Society of Plant Biologists).

Figure 5. Spatiotemporal modelling of hormonal crosstalk correctly predicts auxin patterning in the *aux1* mutant. a and b: Auxin response profiles for wildtype (a) and *aux1* mutant (b). We calculated response profiles using experimental images (Figure 2, Swarup *et al.*, 2001). c and c: The corresponding modelling results of auxin concentration profiles for wildtype (C) and *aux1* mutant (D).

Figure 6. Modelling predictions on the average concentrations of cytokinin and ethylene hormones and the PLS protein. a. Modelling predictions on the average concentrations of cytokinin and ethylene in *pls* mutant, b. Modelling predictions on the average concentrations of PIN protein in PLSox transgenics, *pls*, *etr1* mutants and the *pls etr1* double mutant.

Figure 7. Patterning of PIN1 protein expression. a: Patterning of PIN1 protein by analysing the experimental images (Figure 2, Liu *et al*., 2013). b: Modelling prediction on the patterning of PIN1 protein. The experimental images (Fig. 7a) represent a region in the root from approximately 5 to 25 cell tiers from the tip. In Fig. 7b, this region is denoted by the arrow.

Figure 8. Experimental and modelling results for the patterning of *PLS* gene expression. a: image of *PLS* gene expression. b: PLS protein concentration profile. c: Modelling prediction on PLS protein profile. d: Modelling prediction on PLS protein profile if auxin regulation to *PLS* transcription is removed from hormonal crosstalk network.

Figure 9. A summary on how spatiotemporal modelling of hormonal crosstalk explains the level and patterning of hormones and gene expression in *Arabidopsis thaliana* wildtype and mutant roots.

# THE ROOT

## a. Root Structure

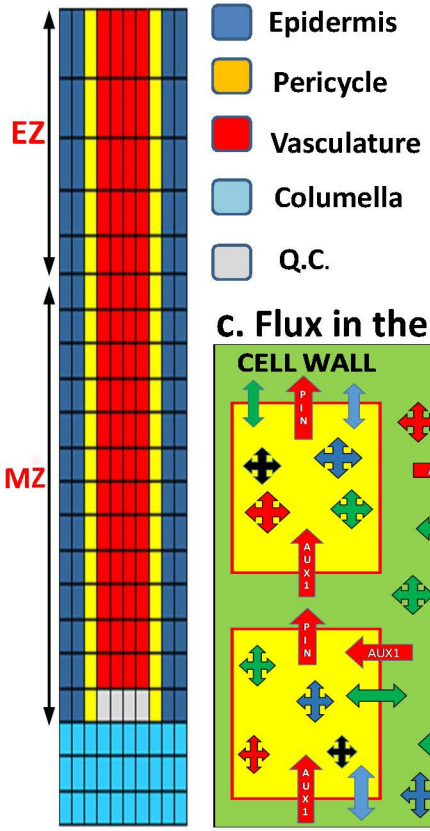


## b. Flux at shoot to root border

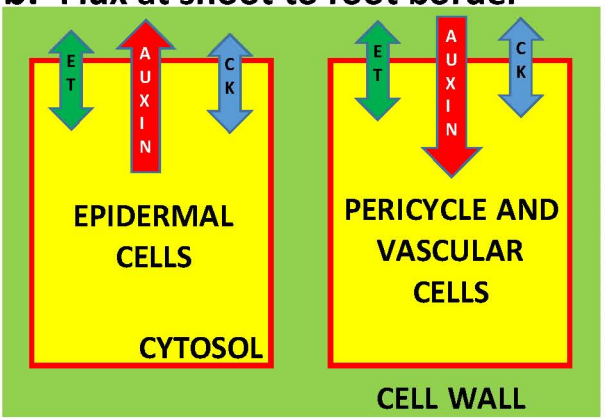


## c. Flux in the root

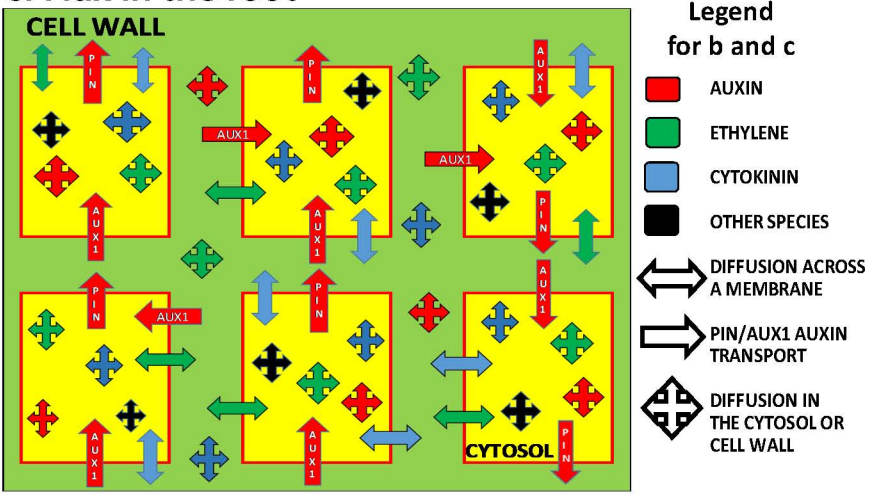


# THE CELL

## d. Crosstalk Network

(see Figure 2)

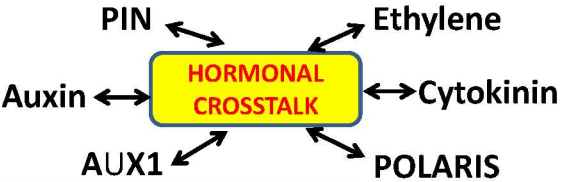


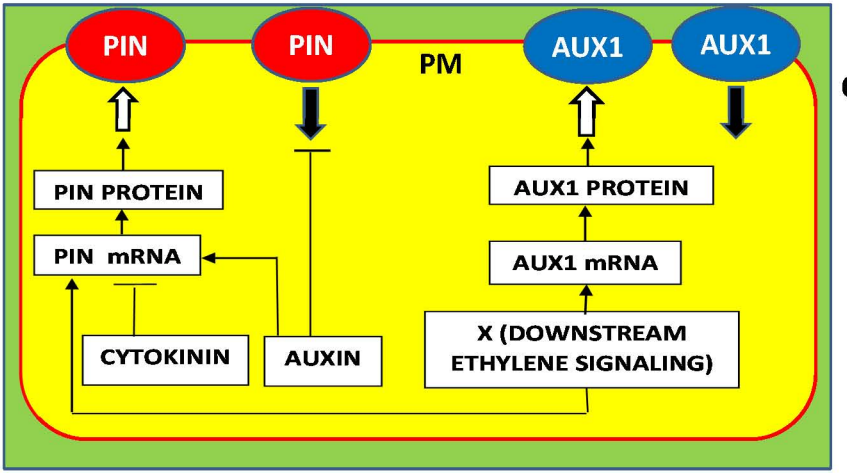


## e. Recycling of auxin carriers PIN and AUX1 to plasma membrane (PM)

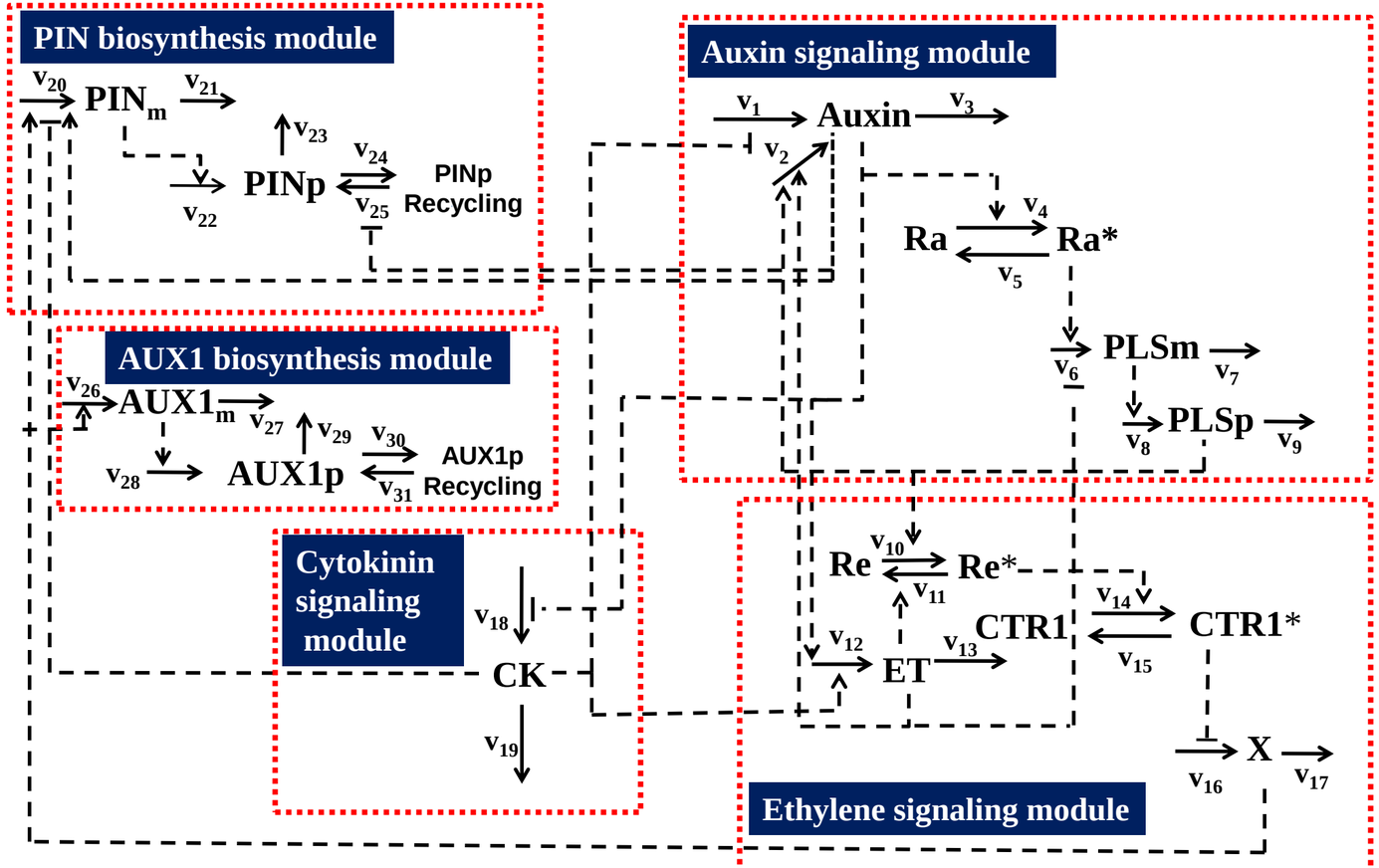
PIN biosynthesis module
v20
PINm
v21
v23
v24
PINp
PINp Recycling
v22
v25
Auxin signaling module
v1
Auxin
v3
v2
v4
Ra
Ra*
v5
PLSm
v6
v7
PLSp
v8
v9
AUX1 biosynthesis module
v26
AUX1m
v27
v29
v30
AUX1p
AUX1p Recycling
v28
v31
Cytokinin signaling module
v18
CK
v19
v10
Re
Re*
v11
v14
CTR1
CTR1*
v12
v13
ET
v15
X
v16
v17
Ethylene signaling module

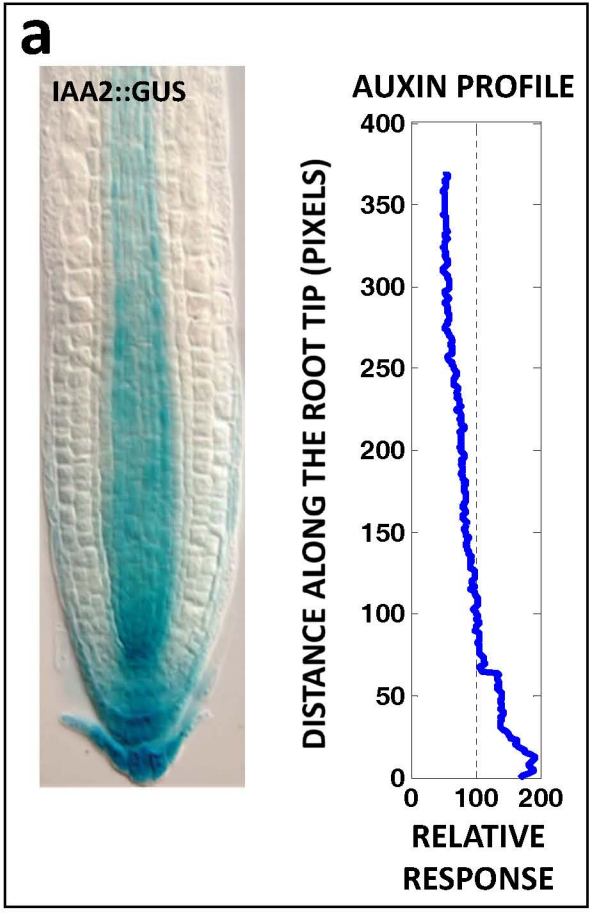
a
IAA2::GUS
AUXIN PROFILE
DISTANCE ALONG THE ROOT TIP (PIXELS)
400
350
300
250
200
150
100
50
0
0
100
200
RELATIVE RESPONSE

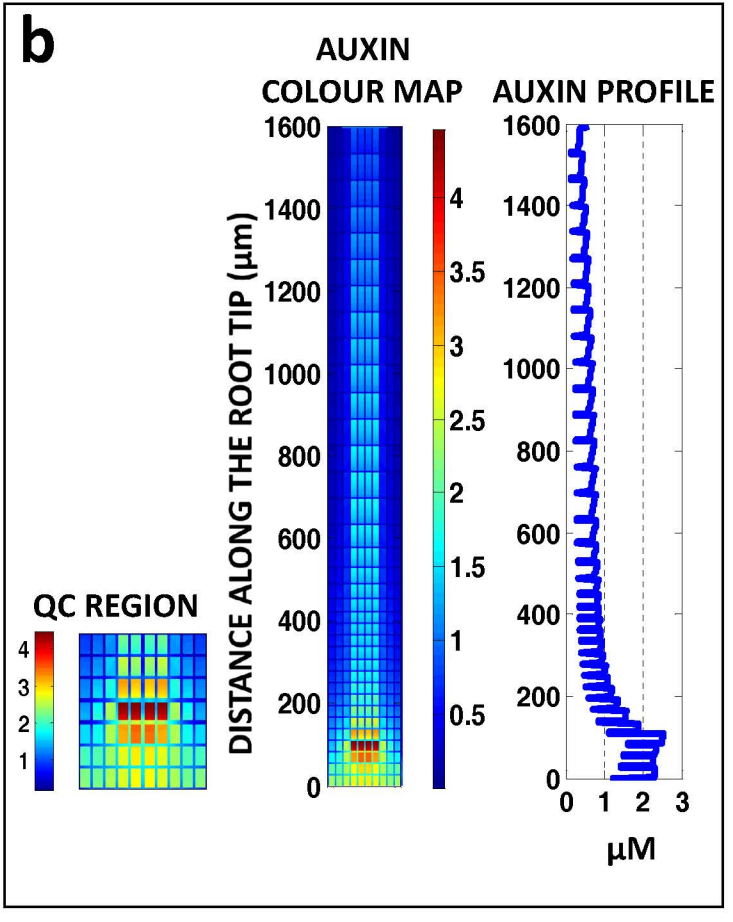
b
AUXIN COLOUR MAP
AUXIN PROFILE
QC REGION
4
3
2
1
DISTANCE ALONG THE ROOT TIP (µm)
1600
1400
1200
1000
800
600
400
200
0
4
3.5
3
2.5
2
1.5
1
0.5
0
1
2
3
µM

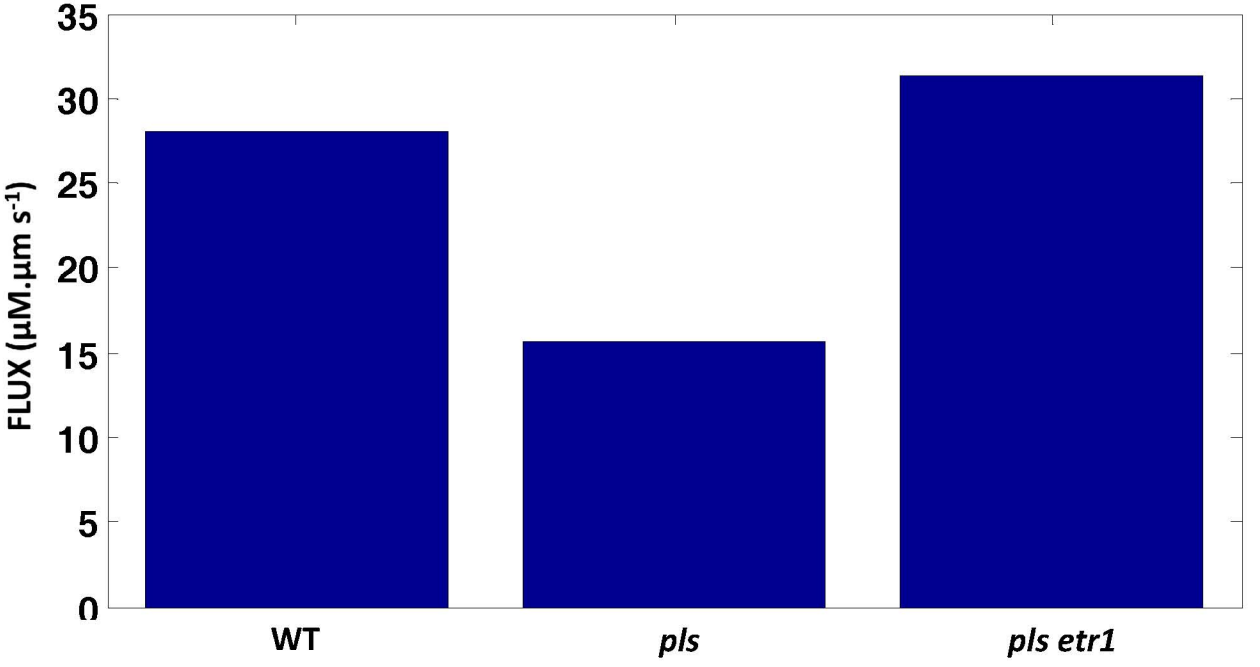
35
30
25
20
15
10
5
0
FLUX (µM.µm s-1)
WT
pls
pls etr1

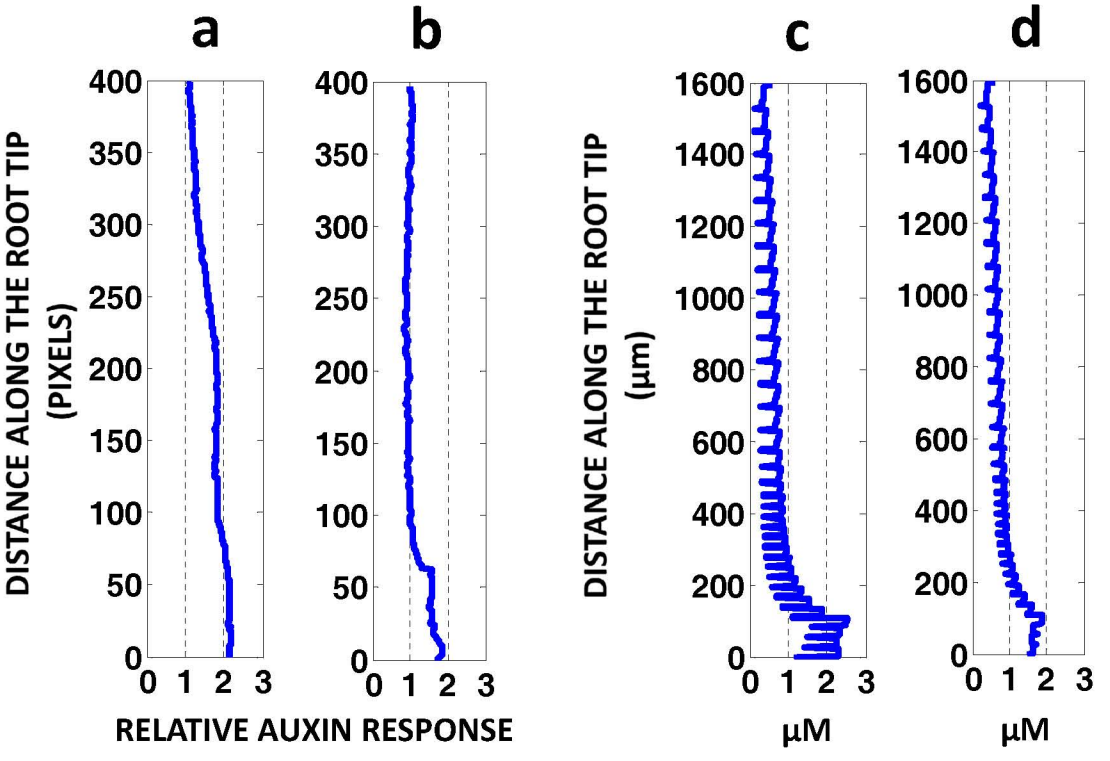
a
b
c
d
DISTANCE ALONG THE ROOT TIP
(PIXELS)
DISTANCE ALONG THE ROOT TIP
(µm)
RELATIVE AUXIN RESPONSE
µM
µM
0
50
100
150
200
250
300
350
400
0
200
400
600
800
1000
1200
1400
1600
0 1 2 3

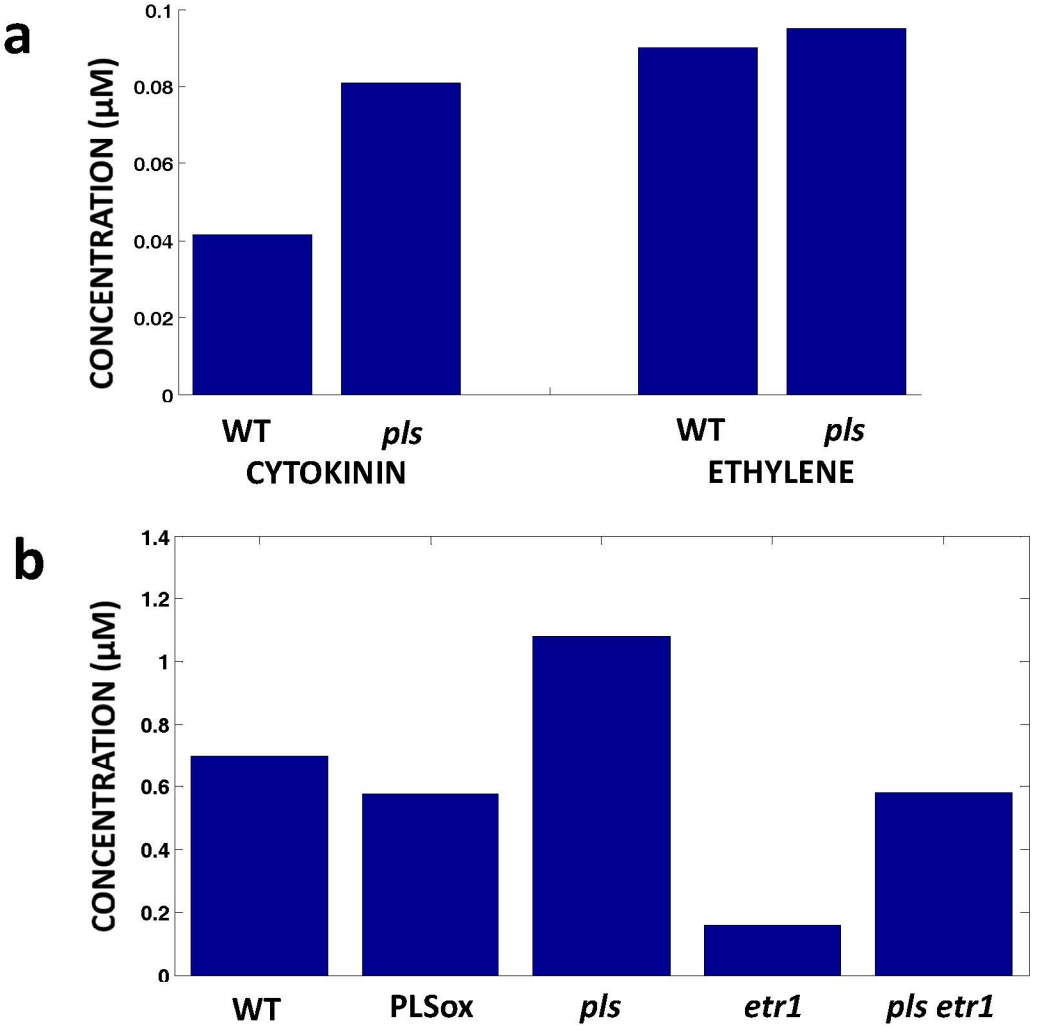
a
CONCENTRATION (µM)
0.1
0.08
0.06
0.04
0.02
0
WT
pls
CYTOKININ
WT
pls
ETHYLENE
b
CONCENTRATION (µM)
1.4
1.2
1
0.8
0.6
0.4
0.2
0
WT
PLSox
pls
etr1
pls etr1

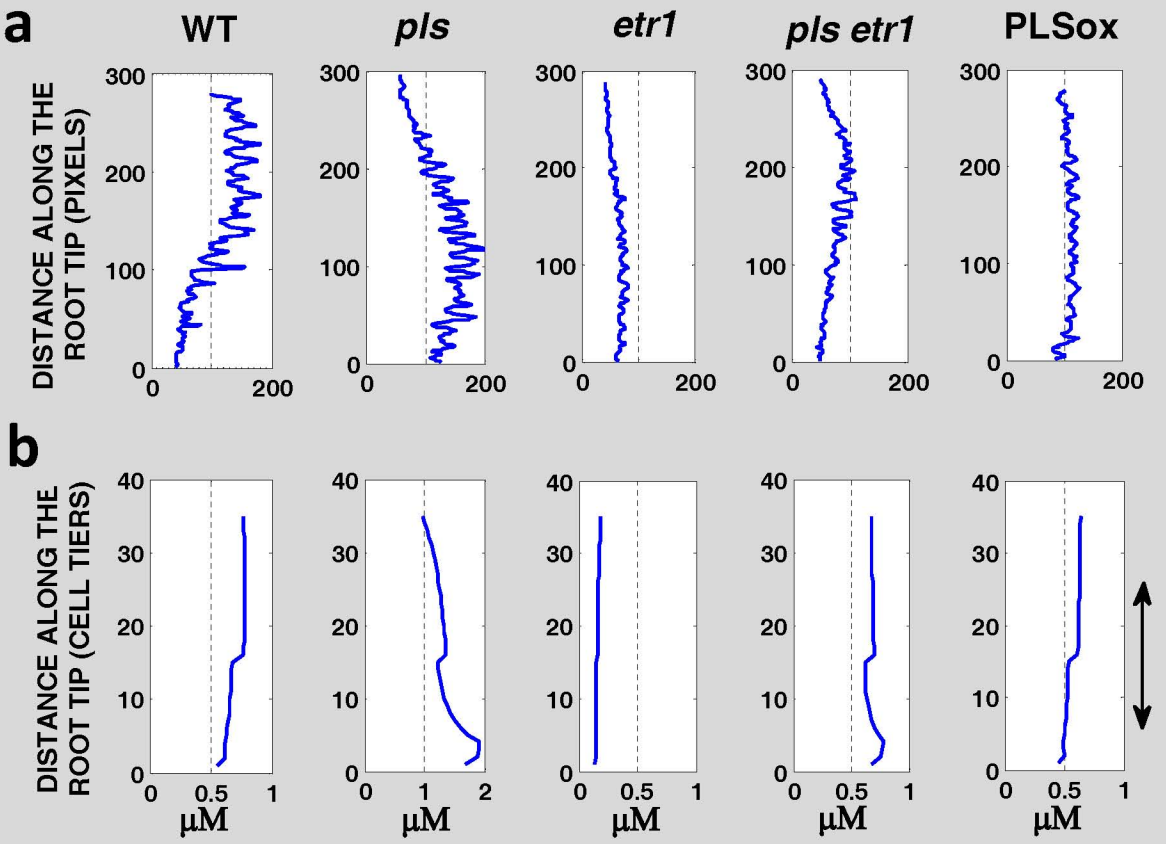
a
WT
pls
etr1
pls etr1
PLSox
DISTANCE ALONG THE ROOT TIP (PIXELS)
300
200
100
0
0
200
b
DISTANCE ALONG THE ROOT TIP (CELL TIERS)
40
30
20
10
0
0
0.5
1
2
µM

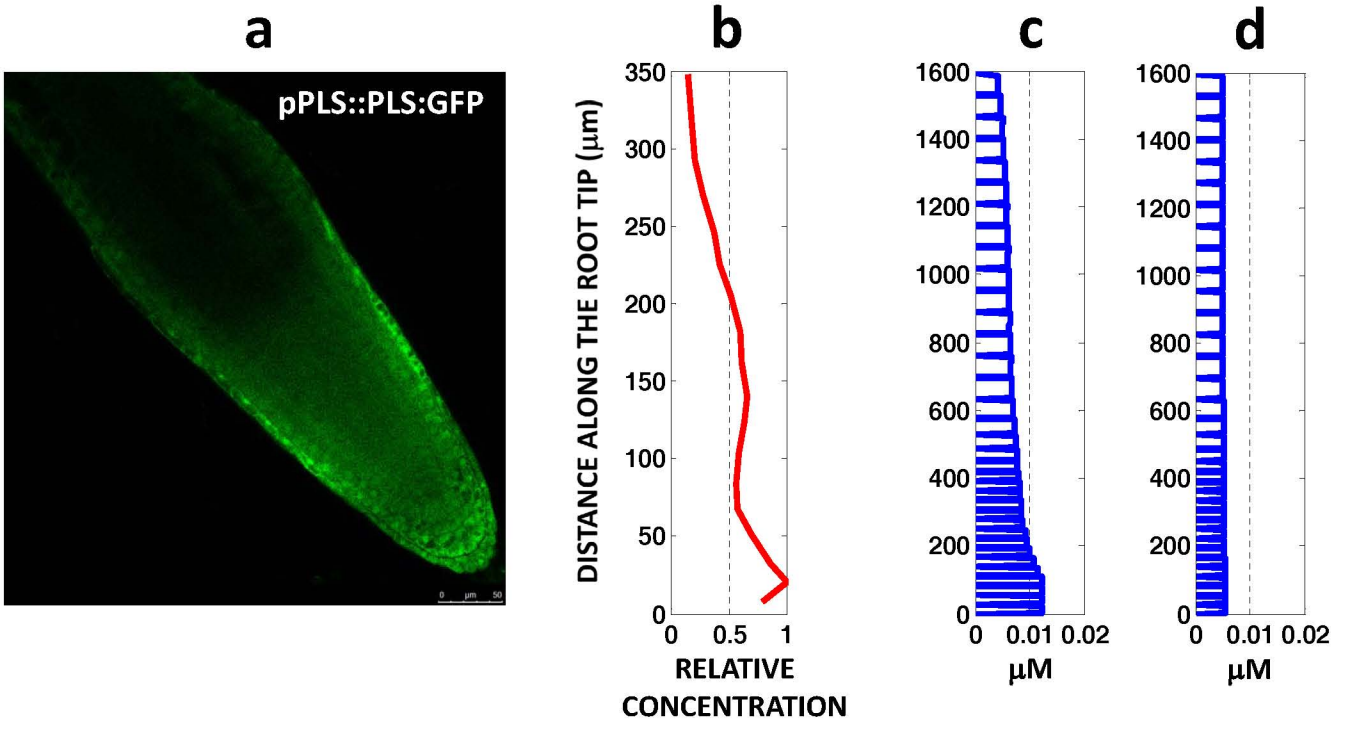
a
pPLS::PLS:GFP
b
c
d
DISTANCE ALONG THE ROOT TIP (µm)
350
300
250
200
150
100
50
0
0
0.5
1
RELATIVE CONCENTRATION
1600
1400
1200
1000
800
600
400
200
0
0
0.01
0.02
µM
1600
1400
1200
1000
800
600
400
200
0
0
0.01
0.02
µM

# HORMONE AND GENE PATTERNING IN THE *ARABIDOPSIS* ROOT TIP IS CONTROLLED BY SPATIOTEMPORAL CROSSTALK OF AUXIN, ETHYLENE, CYTOKININ, PIN, AUX1 AND PLS

**1. MODEL**

- Crosstalk network
- 2-D root structure

→

**2. CALIBRATION**

- Auxin patterning in wild type
- Auxin concentrations in wild type and mutants

→

**3. PREDICTION**

- Levels of ethylene, cytokinin and PIN proteins
- Auxin flux from shoot to root
- Auxin patterning in *aux1* mutant
- PIN patterning
- PLS patterning
- Ethylene patterning